

Constraining rooting depths in tropical rainforests using satellite data and ecosystem modeling for accurate simulation of gross primary production seasonality

KAZUHITO ICHII*, HIROFUMI HASHIMOTO†, MICHAEL A. WHITE‡, CHRISTOPHER POTTER§, LUCY R. HUTYRA¶, ALFREDO R. HUETE||, RANGA B. MYNENI**, RAMAKRISHNA R. NEMANI§

*Ecosystem Science and Technology Branch, NASA Ames Research Center, San Jose State University, Mail Stop 242-4, Moffett Field, CA 94035, USA, †Ecosystem Science and Technology Branch, NASA Ames Research Center, California State University at Monterey Bay, Mail Stop 242-4, Moffett Field, CA 94035, USA, ‡Department of Watershed Science, Utah State University, Logan, UT 84322-5210, USA, §Ecosystem Science and Technology Branch, NASA Ames Research Center, Mail Stop 242-4, Moffett Field, CA 94035, USA, ¶Department of Earth and Planetary Sciences and Division of Engineering and Applied Sciences, Harvard University, Cambridge, MA 02138, USA, ||Department of Soil, Water, and Environmental Science, University of Arizona, Tucson, AZ 85721, USA, **Department of Geography and Environment, Boston University, 675 Commonwealth Avenue, Boston, MA 02215, USA

Abstract

Accurate parameterization of rooting depth is difficult but important for capturing the spatio-temporal dynamics of carbon, water and energy cycles in tropical forests. In this study, we adopted a new approach to constrain rooting depth in terrestrial ecosystem models over the Amazon using satellite data [moderate resolution imaging spectro-radiometer (MODIS) enhanced vegetation index (EVI)] and Biome-BGC terrestrial ecosystem model. We simulated seasonal variations in gross primary production (GPP) using different rooting depths (1, 3, 5, and 10 m) at point and spatial scales to investigate how rooting depth affects modeled seasonal GPP variations and to determine which rooting depth simulates GPP consistent with satellite-based observations. First, we confirmed that rooting depth strongly controls modeled GPP seasonal variations and that only deep rooting systems can successfully track flux-based GPP seasonality at the Tapajos km67 flux site. Second, spatial analysis showed that the model can reproduce the seasonal variations in satellite-based EVI seasonality, however, with required rooting depths strongly dependent on precipitation and the dry season length. For example, a shallow rooting depth (1–3 m) is sufficient in regions with a short dry season (e.g. 0–2 months), and deeper roots are required in regions with a longer dry season (e.g. 3–5 and 5–10 m for the regions with 3–4 and 5–6 months dry season, respectively). Our analysis suggests that setting of proper rooting depths is important to simulating GPP seasonality in tropical forests, and the use of satellite data can help to constrain the spatial variability of rooting depth.

Keywords: Amazon, Biome-BGC, carbon cycle, gross primary production, MODIS, remote sensing, rooting depth, seasonal cycle, terrestrial biosphere model, tropical forest, vegetation index

Received 18 April 2006; revised version received 24 July 2006 and accepted 31 July 2006

Introduction

Tropical forests, which account for about 20% of global terrestrial carbon stocks and 30% of global terrestrial

productivity (Prentice *et al.*, 2001), play important role in the global carbon cycle responding to environmental changes. Although atmospheric observations, ground observations, and ecosystem models are used to understand current changes in tropical forests, there are large uncertainties in current carbon budgets among methods and models (e.g. Schimel *et al.*, 2001; Houghton, 2003). Large uncertainties also remain in understanding

Correspondence: Kazuhito Ichii, c/o Ramakrishna R. Nemani, tel: +1 650 604 6444, fax: +1 650 604 6569, e-mail: kichiijp@yahoo.co.jp

various carbon cycle processes such as gross primary productivity (GPP), respiration, and deforestation (e.g. Clark, 2004; Fearnside, 2004).

GPP, which is one of the important components of the terrestrial carbon cycle, shows large differences between observations and model simulations in terms of controlling processes in tropical evergreen forests. Some ground observations show that carbon uptake peaks near the end of the dry season (Saleska *et al.*, 2003; Goulden *et al.*, 2004). This pattern is partially explained by the seasonal GPP variations that increase during the dry season and peak in the end of the dry season (Goulden *et al.*, 2004) with no sign of drought stress on GPP in the dry season (Rocha *et al.*, 2004; Xiao *et al.*, 2005). Other ground-based studies, however, show depressed photosynthetic activity in the dry season due to moisture stress (Araujo *et al.*, 2002; Malhi *et al.*, 2002). Satellite-based vegetation index (VI) analysis has shown increases in vegetation activity in the dry season (Xiao *et al.*, 2005; Huete *et al.*, 2006). Empirical analyses also suggest that radiation is important for vegetation growth in tropical evergreen forests (Churkina & Running, 1998; Nemani *et al.*, 2003).

On the other hand, results of terrestrial ecosystem models in simulating GPP seasonality largely depend on the model setting. Some terrestrial ecosystem models have failed to simulate seasonal variations in the carbon cycle over tropical evergreen forests. For example, Saleska *et al.* (2003) pointed out that the simulated carbon cycle seasonalities of two ecosystem models were opposite to the ground observations, (i.e. models show carbon uptake in the wet season and release in the dry season), due to strong drought stress on modeled photosynthesis. On the other hand, several studies have successfully simulated seasonal carbon budgets in tropical forests (Kleidon & Heimann, 1998; Potter *et al.*, 2001b).

A main reason for these differences in the results of ecosystem models is the setting of rooting depth. Rooting depth, a parameter for the storage size of the soil water pool, determines the amount of plant available water for transpiration during dry season, and in turn affects the role of water stress on vegetation productivity. Although several studies have reported the role of deep roots for water uptake to maintain green canopies (e.g. Nepstad *et al.*, 1994; Jackson *et al.*, 2000), sustain high evapotranspiration and net primary productivity (NPP) during the dry season (e.g. Kleidon & Heimann, 1998; Zeng *et al.*, 1998; Potter *et al.*, 2001b), it is difficult to obtain the spatial distribution of rooting depth due to the lack of observations. A few studies attempted to estimate spatial rooting depth patterns. For example, Kleidon & Heimann (1998) and Kleidon (2004) estimated the rooting depth by ecosystem model inversions

to maximize NPP or optimize satellite-based absorbed photosynthetically active radiation (APAR). However, their analysis was based on the advanced very high resolution Radiometer (AVHRR), which have measurements contaminated by cloud, water vapor, and aerosols (Kobayashi & Dye, 2005). Huete *et al.*, (2006) have found MODIS data, processed with state-of-the art algorithms for geometric registration, radiometric calibration, and atmospheric corrections, to accurately represent seasonal vegetation dynamics in the Amazonia.

In this study, we adopted an alternative approach to constrain rooting depth in terrestrial ecosystem models in the Amazon River Basin using satellite based analysis (diagnostic analysis) and terrestrial ecosystem model based analysis (prognostic analysis) by simulating the seasonal GPP variation. Using the VI data from the moderate resolution imaging spectroradiometer (MODIS) as a satellite-based data and Biome-BGC as a terrestrial ecosystem model, we simulated seasonal GPP variations with different rooting depths, and discussed how rooting depth affects seasonal GPP variations and which rooting depth simulates GPP consistently with satellite-based observation. In summary, the objectives of the study are (1) to infer the rooting depth of tropical evergreen forests, (2) to assess the capability of satellite-based VI data for monitoring seasonal GPP variations, and (3) to characterize the spatial patterns of inferred rooting depths.

Methods

Study area

Our study focused on Evergreen Broadleaf Forests (EBF) regions in the Amazon River Basin. We used a global land cover map (DeFries *et al.*, 1998), and converted the original 8 km data to 0.5° spatial resolution, identifying pixels with a dominant EBF cover in the Amazon River Basin (Fig. 1). All spatial analysis was done with 0.5° spatial resolution.

Seasonal variations of the climate parameters show regional contrasts in terms of the precipitation and downwelling surface solar radiation (Fig. 2). In general, precipitation mostly peaks in March to May (MAM) and December to February (DJF), and solar radiation peaks in September to November (SON) season over the most of the study area. The Northwestern region has more precipitation and less solar radiation than the other regions and is characterized by weak solar radiation and precipitation seasonality, with a short dry season (0–2 months). Toward the Southeast region the climate is characterized by less precipitation, a longer dry season, more solar radiation, and greater seasonality in precipitation and solar radiation. In the Southeastern

region, the climate has a longer dry season (5–6 months) from June to November with solar radiation peaks in SON.

Model

We used the Biome-BGC version 4.2 model to simulate monthly GPP variations over the tropical evergreen forests in the Amazon River Basin. Biome-BGC prog-

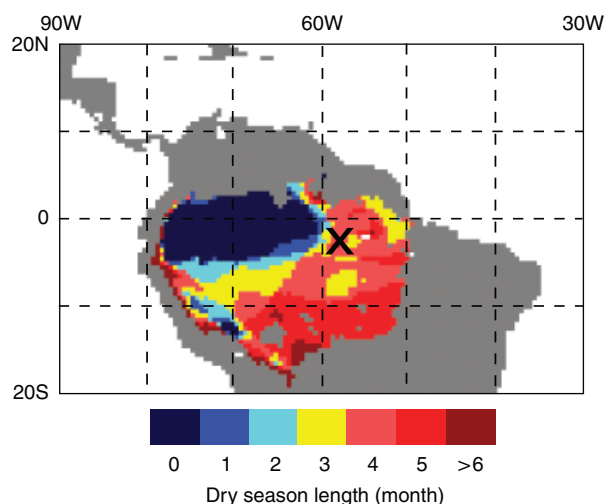


Fig. 1 Study area and spatial patterns in dry season length. Dry season length is defined as the number of months with less than $100 \text{ mm month}^{-1}$ rainfall based on CRU TS2.1 precipitation data from 1984 to 2000. The flux observation site used in the study (Tapajos km67) is marked as X.

nistically simulates the states and fluxes of terrestrial carbon, water, and nitrogen at a daily time step using time-variant climate data (Thornton *et al.*, 2002). GPP is estimated with a combined photosynthetic (Farquhar *et al.*, 1980) and canopy conductance (Jarvis, 1976) model; autotrophic and heterotrophic respirations (AR and HR) are simulated based on the carbon and nitrogen pools with temperature (for AR and HR) and soil moisture status (for HR only).

The model has a one-box soil water pool, and therefore does not include vertical soil water layer, root hydraulic redistribution, and vertical distribution of root density in the extraction and movement of water within the soil profile which are potentially important for tropical forest water cycle modeling (e.g. Lee *et al.*, 2005; Oliveira *et al.*, 2005). Potential impacts of these simplifications on results are discussed in the results and discussion section.

Variations in the input climate parameters affect the carbon cycle in many ways. Briefly, temperature affects photosynthesis through enzyme activity and stomatal conductance and AR and HR by temperature effects on respiration; precipitation affects photosynthesis and HR through soil moisture status; solar radiation directly affects photosynthesis; and vapor pressure deficit (VPD) affects photosynthesis through stomatal conductance. Further Biome-BGC details are described elsewhere (e.g. Thornton *et al.*, 2002; Fujita *et al.*, 2003).

We briefly describe the effects of the rooting depth on GPP in the model here. The setting of the rooting depth determines the vertical extent of the soil water storage accessible to plants, (i.e. deep rooting depth increases

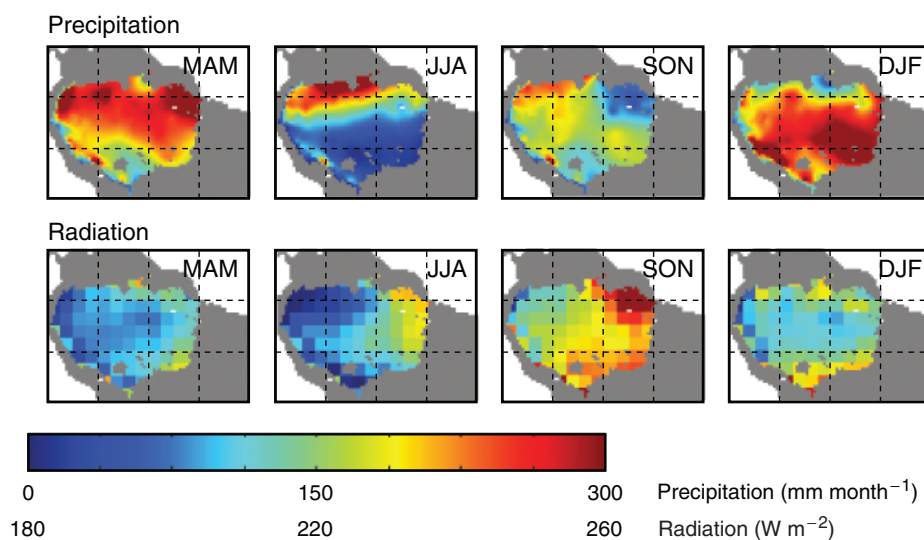


Fig. 2 Seasonal variations [March to May (MAM), December to February (DJF), September to November (SON), and June to August (JJA)] in precipitation and incoming surface solar radiation over the study area. Seasonal averages are based on the CRU TS 2.1 precipitation data and ISCCP-FD downwelling surface solar radiation data from 1984 to 2000.

the soil water holding capacity). Soil water content is calculated by the water balance of precipitation, evapotranspiration, and runoff, and the soil water holding capacity is used to calculate runoff, (i.e. soil water in excess of soil water holding capacity is routed to runoff). Therefore, soils with high water holding capacities can store more water in the wet season in tropical forests, and in turn sustain photosynthesis and evapotranspiration during the dry season. On the other hand, soils with shallow rooting depth cannot hold enough water to sustain the photosynthesis and evapotranspiration during the dry seasons, which leads to soil water stress, stomatal closure, and photosynthesis reduction.

In addition, we incorporated seasonal variations in percent of leaf nitrogen in Rubisco (PLNR) based on the studies of temperate forests, (i.e. PLNR peaks in the middle of growing season Wilson *et al.*, 2000). Based on the results that new leaf flush occurred mostly within the dry season for the field site in Manaus (Roberts *et al.*, 1998), we defined start of new leaf flush season as July. Based on these assumptions, we modeled the seasonal

variability of PLNR as

$$\begin{aligned} \text{PLNR}(d) &= a \sin\left(\frac{d}{365}2\pi\right) + \text{PLNR}_{\text{base}} \quad (d \geq 182), \\ \text{PLNR}(d) &= a \cos\left(\frac{365-d}{365}2\pi\right) + \text{PLNR}_{\text{base}} \quad (d < 182), \end{aligned} \quad (1)$$

where a is amplitude of seasonal PLNR variations (we set $a = 0.015$), d is the day of the year since the beginning of the year, and $\text{PLNR}_{\text{base}}$ is minimum PLNR (which corresponds with PLNR in the beginning and end of the growing season). Incorporation of this dynamic parameter in the model produces higher GPP in the beginning of wet season when radiation declines, which is consistent with flux tower-based GPP.

As the model input parameter, we used the ecophysiological parameters shown in Table 1 (e.g. Ichii *et al.*, 2005). Nitrogen deposition and atmospheric CO_2 concentrations are set $0.0018 \text{ g N m}^{-2} \text{ yr}^{-1}$ (Holland *et al.*, 1999), and 360 ppm, respectively. Other inputs required to run the model are soil texture (Zobler, 1986), elevation (ETOPO-5), and albedo (Dorman & Sellers, 1989).

Table 1 Ecophysiological parameters of evergreen broadleaf forests used in the study

Value	Unit	Description
0.5	1 year^{-1}	Annual leaf and fine root turnover fraction
0.70	1 year^{-1}	Annual live wood turnover fraction
0.03	1 year^{-1}	Annual whole-plant mortality fraction
1.2	Ratio	(Allocation) new fine root C: new leaf C
2.2	Ratio	(Allocation) new stem C: new leaf C
0.16	Ratio	(Allocation) new live wood C: new total wood C
0.22	Ratio	(Allocation) new croot C: new stem C
42.0	kg C (kg N)^{-1}	C:N of leaves
55.0	kg C (kg N)^{-1}	C:N of leaf litter, after retranslocation
48.0	kg C (kg N)^{-1}	C:N of fine roots
50.0	kg C (kg N)^{-1}	C:N of live wood
550.0	kg C (kg N)^{-1}	C:N of dead wood
0.38	DIM	Leaf litter labile proportion
0.44	DIM	Leaf litter cellulose proportion
0.18	DIM	Leaf litter lignin proportion
0.34	DIM	Fine root labile proportion
0.44	DIM	Fine root cellulose proportion
0.22	DIM	Fine root lignin proportion
0.77	DIM	Dead wood cellulose proportion
0.23	DIM	Dead wood lignin proportion
0.01	$1 \text{ LAI}^{-1} \text{ day}^{-1}$	Canopy water interception coefficient
0.54	DIM	Canopy light extinction coefficient
15.0	$\text{m}^2 (\text{kg C})^{-1}$	Canopy average specific leaf area (projected area basis)
0.02	DIM	Fraction of leaf N in Rubisco
0.006	m s^{-1}	Maximum stomatal conductance (projected area basis)
-0.34	MPa	Leaf water potential: start of conductance reduction
-2.2	MPa	Leaf water potential: complete conductance reduction
1100.0	Pa	Vapor pressure deficit: start of conductance reduction
3600.0	Pa	Vapor pressure deficit: complete conductance reduction
0.18	kg C (kg N)^{-1}	Specific respiration rate

Data

Flux tower based data. We used flux tower based climate data as model input and GPP for validation in an old growth seasonally wet tropical evergreen forest, located in the Tapajos National Forest km67 (2°51'24"S, 54°57'32"W), Para, Brazil (Fig. 1; Saleska *et al.*, 2003). All of the original data are provided hourly, and we converted them into daily or monthly means.

The climate data required to run the model are daily data of maximum and minimum temperature, precipitation, VPD, and solar radiation. Daily maximum and minimum temperature and precipitation are obtained from hourly observations of temperature and precipitation. We calculated VPD based on the assignment of daily minimum temperature as dew point temperature (Campbell & Norman, 1998), and solar radiation by converting photosynthetic photon flux density (PPFD) using an average energy for PAR photon ($4.55 \mu\text{molJ}^{-1}$).

Flux tower based hourly GPP is calculated as $R_{\text{tot}} - \text{NEE}$, where R_{tot} is total ecosystem respiration and NEE is net ecosystem exchange. R_{tot} equals NEE at night and is assumed to have the same average value during the day as at night. Detailed data processing for the gap-filling and GPP calculations are described in Saleska *et al.* (2003). We calculated the monthly total GPP using original hourly data from 2002 to 2004.

Gridded climate data. As climate inputs for spatial model simulation, we used daily maximum and minimum temperature, precipitation, VPD, and solar radiation from 1984 to 2000. Daily maximum and minimum temperatures were derived from National Centers for Environmental Prediction (NCEP) reanalysis data sets (Kalnay *et al.*, 1996). We adjusted daily NCEP precipitation data using monthly Climate Research Unit (CRU) TS2.1 precipitation data (Mitchell & Jones, 2005) while preserving the frequency of rainy days in each grid cell. Daily VPD is calculated from surface pressure, specific humidity, and temperature from the NCEP data sets. We adjusted daily NCEP solar radiation data using monthly solar radiation data from the International Satellite Cloud Climatology Project Radiation Flux profile (ISCCP-FD) data set (Zhang *et al.*, 2004).

Satellite based VI data. We used normalized difference VI (NDVI) and enhanced VI (EVI) data in the MODIS VI products (MOD13A2) from 2001 to 2004 (Huete *et al.*, 2002). The products are provided at 1 km spatial resolution and 16 day compositing periods using MODIS surface reflectance products (MOD09), which are atmospherically corrected for molecular scattering,

ozone absorption, and aerosols (Vermote *et al.*, 2002). Although NDVI is the most commonly used VI, several limitations including saturation in closed dense canopies and high sensitivity to both atmospheric aerosols and the soil background are reported (e.g. Huete *et al.*, 2002). On the other hand, EVI was developed to optimize the vegetation signal with improved sensitivity in high biomass regions and improved vegetation monitoring through a decoupling of the canopy background signal and a reduction in atmospheric influences including blue band for reducing atmospheric contamination (Huete *et al.*, 2002).

For the point analysis, we used $7 \text{ km} \times 7 \text{ km}$ pixels centered on a flux tower site. We used the pixels which satisfy the following four standards in the VI quality assurance (QA) science data sets in MOD13A2 products; (1) VI quality is 'VI produced with good quality' or 'VI produced but with unreliable quality and examination of other QA bits recommended,' (2) VI usefulness index is better than 'fair quality,' (3) mixed clouds flag is 'no mixed clouds,' and (4) shadow flag is 'no shadow.' We calculated an average 16 day VI if the number of selected pixels exceeds 10% of the corresponding $7 \text{ km} \times 7 \text{ km}$ region, and computed monthly averages by temporal weighting, and calculated monthly variations by averaging 4 years data for both NDVI and EVI.

For the spatial analysis, we used 12 MODIS tiles to cover the study area. First, we averaged over 0.5° spatial resolution using the selected pixels in each 16 day product. We used the same standard as the point analysis to select the data for spatial averaging. Then, we produced monthly averages by temporal weighting. Lastly, we averaged over 4 years to produce the averaged monthly variations in NDVI and EVI.

Experiments

In this study, the analysis consists of the point analysis at Tapajos km67 flux site, and the spatial analysis over the Amazon River Basin. First, we conducted a point-based analysis to validate the modeled GPP seasonality, then we analyzed the sensitivity of GPP to the setting of rooting depth, and finally we tested the capability of satellite-based VIs to infer the GPP seasonality. We extended this to the spatial analysis using the satellite-based VI data as a surrogate of GPP.

Point analysis. First, we validated the model and tested the sensitivities of modeled GPP seasonality to rooting depth settings at the Tapajos km67 flux site. Using the daily climate input from 2002 to 2004, we executed the model to simulate seasonal GPP variation based on

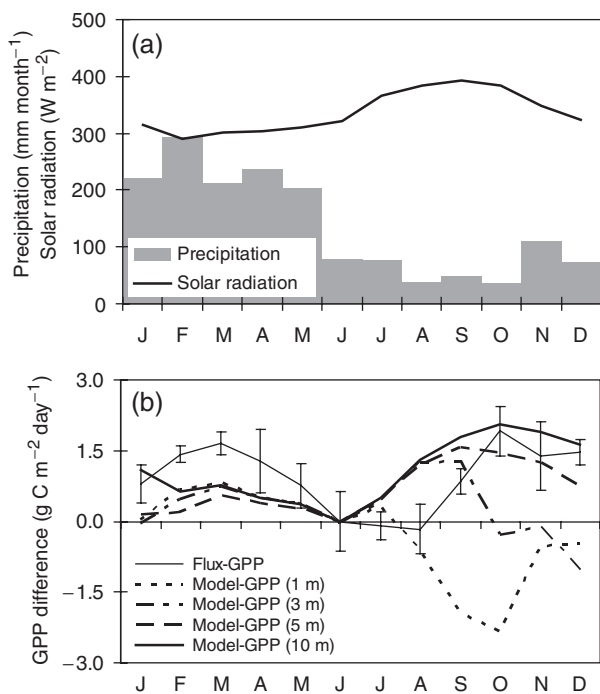


Fig. 3 Monthly variations in (a) climate parameters (precipitation and radiation), and (b) flux-based and modeled gross primary production (GPP) at Tapajos km67 flux tower site under different rooting depth (1, 3, 5, and 10 m) averaged over 2002–2004. Error bars in flux-based GPP show the standard deviation of 3 years' monthly data. GPP differences from June are plotted. Positive GPP difference shows positive anomaly of carbon fixation by vegetation.

different rooting depth inputs. For the model spinup, the model was run until the soil carbon pool reaches near equilibrium, then was executed using the data for 2002 to 2004. To analyze the sensitivities of GPP seasonality to rooting depth settings, we adopted four rooting depths of 1, 3, 5 and 10 m. One meter rooting depth is one of the common values in terrestrial ecosystem modeling (e.g. Kleidon & Heimann, 1998), and close to the mean depth above which 95% of all roots are located in the soil (Schenk & Jackson, 2002). In addition, we used 3, 5 and 10 m rooting depths, as several studies reported deep rooting depths and their roles in tropical forests (e.g. Nepstad *et al.*, 1994; Canadell *et al.*, 1996; Kleidon & Heimann, 1998). Then, using flux tower based GPP and satellite-based VIs (EVI and NDVI), we selected the suitable VI to represent seasonal GPP patterns for the spatial analysis.

Spatial analysis. We analyzed the seasonal variations in modeled GPP and satellite-based VIs over the study area to test how satellite-based data can constrain rooting depths in ecosystem models for tropical

evergreen forests. For the model run, spin-up was done using the data from 1984 to 2000 until soil carbon became equilibrium at each grid, then the model was executed. Monthly GPP was calculated by averaging entire period. To analyze the sensitivity of seasonal GPP variations to the rooting depth, we compared the modeled seasonal GPP variations with satellite-based VI. All of the results were standardized by taking anomaly from May average, as water limitation has small impacts on the carbon cycles in the end of the rainy season (May in most of the study areas; Fig. 1).

Results and discussion

Point analysis

Sensitivity of GPP seasonality to the rooting depth. At Tapajos km67 flux tower site, the mean dry season extends from approximately July 15 to December 15 (e.g. Saleska *et al.*, 2003; Hutrya *et al.*, 2005), and solar radiation peaks in September and October for 3 years' average from 2002 to 2004 (Fig. 3a). Flux-based GPP is lowest in June, July and August due to the ecosystem preparing for leaf senescence (e.g. Goulden *et al.*, 2004), and increases until October which corresponds to the peak radiation (Fig. 3b). GPP has its maximum values from October to March (from the middle of dry season to the middle of the wet season), and then declines. The GPP increases in the dry season indicate weak or no drought stress for photosynthesis, which is consistent with other studies based on flux observations (Goulden *et al.*, 2004) and satellite-based observations (Xiao *et al.*, 2005; Huete *et al.*, 2006).

Modeled GPP shows a high sensitivity of GPP to the rooting depth settings (Fig. 3b), and only the assumption of deep rooting system (e.g. 10 m) can capture the flux-based GPP seasonality. For the rooting depth 1 m simulation, GPP shows a strong decline due to a strong drought stress impact on photosynthesis during the dry season, which is not consistent with flux GPP. The 3 m rooting depth simulation shows GPP increases in the beginning of dry season, however, GPP declines in the end of the dry season due to the drought stress. The 5 m rooting depth simulation extends the length of GPP increases in the dry season. However, GPP declines in the end of the dry season significantly due to the drought stress that is inconsistent with flux GPP. Only 10 m rooting depth successfully tracks the flux-based GPP seasonality during the dry season and the beginning of wet season.

Use of satellite VI for GPP. In order to test the capability of satellite based VI data to monitor GPP, the correlation

between monthly VIs and flux-based GPP were analyzed. The correlation between EVI and GPP is much higher ($R^2 = 0.46$) than that of NDVI-GPP ($R^2 = 0.03$) with linear regression results of $GPP = 11.7EVI + 2.1$, and $GPP = -3.9NDVI + 11.9$. These contrasting relationships are explained by the advantages of EVI; the EVI is sensitive even in high LAI canopies by relying on near-infrared reflectance and resistant with atmospheric noise by including blue band reflectance (Huete *et al.*, 1997, 2002). Empirical analysis suggests that EVI can be used to track GPP seasonality, therefore we used EVI as a surrogate of GPP for the spatial analysis (Huete *et al.*, 2006).

Spatial analysis

EVI spatial – seasonal variations are roughly similar to that of solar radiation variations (Figs 2 and 4). In June to August (JJA), EVI and solar radiation are minimum over the study area. Then, EVI peaks in SON corresponding with maximum solar radiation. In contrast to seasonal patterns in precipitation, the EVI is minimum in MAM and JJA and maximum in SON and DJF through most of the Amazon regions, suggesting no or weak drought effects on photosynthesis in the dry season.

Seasonal patterns in modeled GPP are sensitive to the setting of the rooting depth and the seasonal precipita-

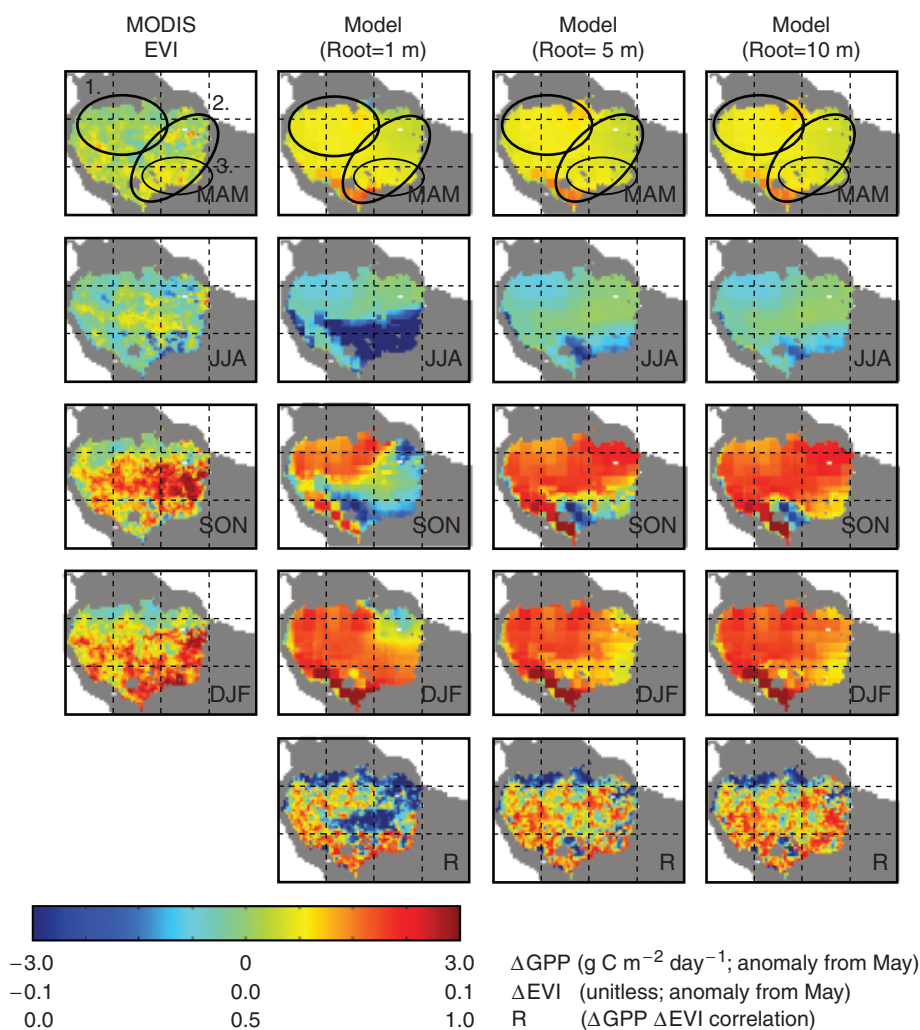


Fig. 4 Seasonal [March to May (MAM), June to August (JJA), September to November (SON), and December to February (DJF)] variations in simulated gross primary production (GPP) under different rooting depth (1, 5, and 10 m) and satellite-based enhanced vegetation index (EVI), and correlation coefficients (R) of monthly variations of EVI and GPP. Averages from 1984 to 2000 for GPP and from 2001 to 2004 for EVI are calculated, and anomalies from May are shown. Positive ΔGPP shows positive anomaly of carbon fixation by vegetation. Three regions (shown as ovals in MAM) are defined to characterize the sensitivity of GPP to rooting depth (See text).

tion pattern especially in dry season (Fig. 4). For example, for the 1 m rooting depth simulation, most of the southern areas show large GPP decreases in JJA and SON seasons due to the strong drought stress in the dry season. A deeper rooting depth setting creates a weaker drought stress in the dry season (i.e. 5 m setting show a smaller negative anomaly in the southeastern regions in JJA and SON seasons). In addition, the higher sensitivity of GPP to the rooting depth is seen in the regions with the longer dry season [i.e. southern regions which show the highest sensitivity to the rooting depth are characterized by the longest dry season (5–6 months) in the study areas (Figs 1 and 4)]. There are no substantial difference in Δ GPP in middle and end of wet seasons (MAM) when abundant soil water are available.

We summarized the regional dependency of GPP sensitivity on rooting depth and its consistency with EVI by dividing the study areas into three regions (Fig. 4). In region 1, all of three experiments simulated the same GPP seasonality and similar EVI-GPP correlations regardless of the rooting depth settings, which peaks in SON and DJF when radiation takes its maximum and negatively peaks in JJA when radiation takes its minimum, which is consistent with EVI seasonality. These regions are characterized by high precipitation throughout a year with short dry seasons (0–2 months), and only shallow rooting depths are required to support GPP during the dry season. In region 2, GPP under 1 m rooting depth shows different seasonal variations with other rooting depth settings and satellite-based observations, showing strong modeled GPP declines in JJA and SON seasons (dry season) and low EVI-GPP correlations. Both 5 and 10 m rooting depth simulations show that GPP seasonal variations are consistent with EVI, which peaks in SON and shows high EVI-GPP correlations. In region 3, the different settings of the rooting depth affect GPP seasonality most significantly. For 1 m rooting depth, GPP takes its minimum for the whole dry seasons (e.g. through JJA and SON), and recovers in the beginning of the wet season. For 5 m rooting depth, simulated GPP in the SON does not show any positive anomalies, which is inconsistent with EVI. Only GPP with 10 m rooting depth setting is consistent with EVI, which peaks in the SON and DJF. Highest correlation of EVI-GPP monthly variation among three different setting of rooting depth also support that 10 m rooting depth setting is the most appropriate to simulate GPP seasonality in the region 3.

Detailed analysis of monthly GPP and EVI variations based on the ranges of dry season length suggested that the rooting depth required to sustain the consistent seasonal patterns with EVI depends on the length of the dry season (Fig. 5). In very wet regions (e.g. 0–2 month dry season), seasonal variations in modeled GPP

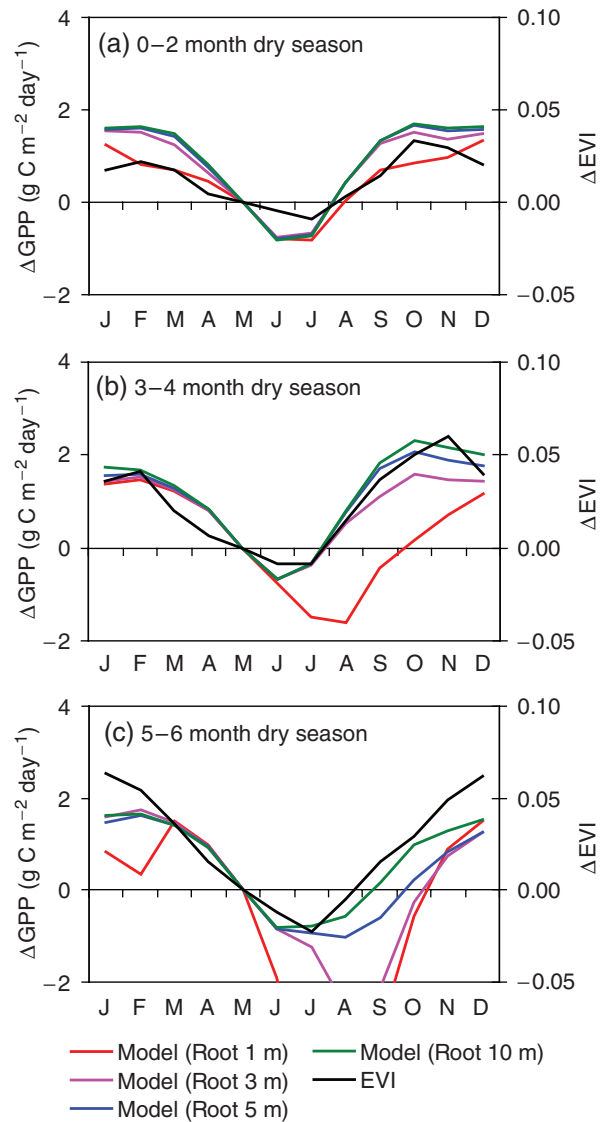


Fig. 5 Monthly variations in simulated GPP under different rooting depth (1, 3, 5, and 10 m) and MODIS enhanced vegetation index (EVI) averaged over the regions with (a) 0–2, (b) 3–4, and (c) 5–6 month dry season in the study area. Anomalies from May are shown for both GPP and EVI. Positive Δ GPP shows positive anomaly of carbon fixation by vegetation.

are not sensitive to the settings of rooting depth and consistent with EVI seasonality. In this region, a shallow rooting depth (1–3 m) is enough to sustain the seasonal EVI patterns (Fig. 5a). In the regions with 3–4 month dry season, simulated GPP based on rooting depths greater than 5 m shows similar patterns with EVI, however, for example, 1 m rooting depth setting shows negative peak of GPP in July and August, which lags 1 month behind EVI due to the strong drought stress. In these regions, 3–5 m rooting depth is required. For the regions with 5–6 month dry season, shallow rooting depth simulation

clearly underestimates the GPP in the dry season, which shows a large decline from June to October (for 1 m rooting depth simulation), and August to October (for 3 m rooting depth simulation). Five meter rooting depth simulation also shows the different peaks in GPP, which lags 2 months in GPP simulations. These analyses show the inferred rooting depth is strongly determined by the seasonal precipitation patterns and length of the dry season.

Comparison of rooting depth with other studies

We compared rooting depths inferred in this study with others. We used two existing data sets of rooting depth; Schenk & Jackson (2002), and Kleidon (2004), and one probability map of deep rooting system (Schenk & Jackson, 2005). Schenk & Jackson (2002) generated a global rooting depth map using observed biomass rooting profiles with nonlinear regression of climate parameters in each vegetation class (hereafter, SJ2002). We used mean 95% ecosystem rooting depth (rooting depth that contains 95% of all roots). Kleidon (2004) generated plant available water maps based on an inverse method using a terrestrial ecosystem model by fitting to satellite-based APAR (hereafter, K2004-1) and maximizing NPP (hereafter K2004-2). As K2004-1 and K2004-2 data are provided as plant available water (mmH₂O), we converted to the rooting depth using field capacity and wilting point (we assumed that the amount of water at wilting point is equivalent to and corresponds to the leaf water potential at stomatal closure (we used -2.2 MPa; Table 1)). Then, average rooting depths are calculated in each region of 0–2, 3–4, and 5–6 months dry season.

Although the general characteristics of rooting depth which increases toward the drier regions (longer dry seasons) are qualitatively consistent among all rooting depth estimations (SJ2002, K2004-1, 2) and empirical analysis of probability of deep rooting system (Schenk & Jackson, 2005), our approach is generally deeper than

other studies (Table 2). First, consistent with Kleidon (2004), estimated rooting depths are much deeper than the SJ2002's estimation especially in the regions with the longer dry seasons (e.g. 3–4 and 5–6 months dry season). As the deepest 5% of roots may supply enough water to sustain transpiration in the dry season (e.g. Nepstad *et al.*, 1994), rooting depth which is based on the 95% of rooting biomass is shallow. Differences with K2004-1 and K2004-2 data may be explained by the model setting (empirical parameterization of water stress for net primary production in Kleidon & Heimann, 1998 model vs. process based parameterization in Biome-BGC), and input parameters (ECMWF precipitation data for Kleidon, 2004 and CRU precipitation data for this study), and the degree of model validations.

Limitation and further model improvements

Although our study successfully simulated the GPP seasonality in Amazon tropical rainforests, we need to point out several limitations of the study. First, the assumption of one box soil water layer in Biome-BGC tends to overestimate the soil water evaporation, underestimate the runoff due to ignoring vertical water transport, and underestimate the water stress for photosynthesis due to the lack of vertical distribution of water and roots. However, these effects are not important in this study. First, overestimation of soil water evaporation due to single soil water layer does not have a large impact on closed canopy tropical forests. Second, as runoff occurs mostly in the wet season, impact on our rooting depth estimation, which is largely determined by length and precipitation amount of dry season, is small. Third, underestimation of the water stress for photosynthesis due to the lack of vertical distribution of water and roots may be partially compensated by hydraulic redistribution (Oliveira *et al.*, 2005). Inclusion of vertical distribution of water and roots potentially increases water stresses for photosynthesis at certain levels of soil layer in dry season. As the current model results capture GPP seasonality consistently with EVI, further water stresses are unlikely. Along with importance of hydraulic redistribution to avoid vegetation water stresses during the dry season (e.g. Oliveira *et al.*, 2005), possible explanation is that our simplification of lack of both vertical distribution of water and roots and hydraulic redistribution rather works appropriately in tropical rainforests.

Second, more accurate information on soil texture and its effects on soil moisture status are required to give further constraints to the rooting depth estimation. Several studies showed the effects of soil texture to the leaf water potential, which potentially affect canopy photosynthesis (e.g. Williams *et al.*, 2002), and to the

Table 2 Estimated rooting depths (units, m) in the study area

Dry season length (months)	This study	SJ2002	K2004-1	K2004-2
0–2	1–3	0.9	1.0	0.9
3–4	3–5	1.2	2.4	2.5
5–6	5–10	1.6	2.7	2.7

SJ2002, K2004-1, and K2004-2 denote Schenk & Jackson (2002), Kleidon (2004) (fitting to satellite-based APAR), and Kleidon (2004) (maximizing NPP) methods.

APAR, absorbed photosynthetically active radiation; NPP, net primary productivity.

empirical estimation of rooting depths (Schenk & Jackson, 2005). Some ecosystem model studies used more detailed information on soil texture and its hydraulic conductivities (e.g. Potter *et al.*, 2001a, b).

Third, the modeling of ecosystem respiration is required to simulate NEE. Field observations showed the importance of seasonal variations in ecosystem respirations responding to the water availabilities (e.g. Saleska *et al.*, 2003; Vourlitis *et al.*, 2005). Current ecosystem models mostly fail to simulate the seasonality of respiration, therefore, further improvements of water effects on respiration are required to simulate NEE.

Conclusion

Combined analysis of satellite-based VI and terrestrial ecosystem model gave constraints on the rooting depths of tropical forests in Amazon. A series of the sensitivity studies showed that GPP seasonality of the tropical forests is sensitive to the setting of rooting depth in the areas with long dry seasons. At Tapajos km67 flux site, we confirmed that setting of rooting depth strongly controls modeled GPP seasonal variations and only models with deep rooting system (e.g. 10 m) can successfully track flux-based GPP seasonality in the dry season. We also showed that satellite-based EVI seasonality can be used as a surrogate of GPP. The spatial analysis showed that the model reproduced the similar GPP seasonality with that of satellite-based EVI; however, required rooting depths are strongly dependent on the precipitation and the dry season length. For example, shallow rooting depth (1–3 m) is required for the regions with short dry season (e.g. 0–2 months), and deeper ones are required in the regions with longer dry seasons (e.g. 3–5 and 5–10 m for the regions with 3–4 and 5–6 months dry season, respectively). Our analysis shows that setting of the rooting depth is important to simulate GPP seasonality in tropical forests, and the use of satellite data can help to constrain the spatial variability of rooting depth.

Our analysis suggests that the reanalysis of the ecosystem models using the deep rooting system is required to project the impacts of the carbon cycle of the tropical forests responding to the future environmental changes. Assumption of the shallow rooting depth which is generally used in the tropical forests ecosystem modeling might overestimate the responses of carbon cycle of the tropical forests (e.g. Amazon rainforest dieback; Cox *et al.*, 2000) to the future precipitation and soil moisture changes. Our analysis suggests that currently most of the tropical evergreen forests regions in Amazon River Basin sustain the photosynthesis through deep rooting systems, which implies GPP is less sensitive to the water availability. Less sensitive

effects of precipitation on the tropical forests GPP might delay the changes of tropical ecosystems responding to the future environmental changes.

Acknowledgement

Funding from NASA's Science Mission Directorate through EOS (K. Ichii, H. Hashimoto, R. R. Nemani) and NASA New Investigator Programs (M. A. White) facilitated this research.

References

- Araujo AC, Nobre AD, Kruijt B *et al.* (2002) Comparative measurements of carbon dioxide fluxes from two nearby towers in a central Amazonian rainforest: the manaus LBA site. *Journal of Geophysical Research*, **107**, 8090, doi: 10.1029/2001JD000676.
- Campbell GS, Norman JM (1998) *Environmental Biophysics*. Springer-Verlag, New York, NY.
- Canadell J, Jackson RB, Ehleringer JR *et al.* (1996) Maximum rooting depth of vegetation types at the global scale. *Oecologia*, **108**, 583–595.
- Churkina G, Running SW (1998) Contrasting climatic control on the estimated productivity of different biomes. *Ecosystems*, **1**, 206–215.
- Clark DA (2004) Tropical forests and global warming: slowing it down or speeding it up? *Frontiers in Ecological Environment*, **2**, 73–80.
- Cox PM, Betts RA, Jones CD *et al.* (2000) Acceleration of global warming due to carbon-cycle feedbacks in a coupled climate model. *Nature*, **408**, 184–187.
- DeFries RS, Hansen M, Townshend JRG *et al.* (1998) Global land cover classifications at 8 km spatial resolution: the use of training data derived from Landsat imagery in decision tree classifiers. *International Journal of Remote Sensing*, **19**, 3141–3168.
- Dorman JL, Sellers PJ (1989) A global climatology of albedo, roughness length and stomatal resistance for atmospheric general circulation models as represented by the simple biosphere model (SiB). *Journal of Applied Meteorology*, **28**, 833–855.
- Farquhar GD, von Caemmerer S, Berry JA (1980) A biochemical model of photosynthesis CO₂ assimilation in leaves of C3 species. *Planta*, **149**, 78–90.
- Fearnside PM (2004) Are climate change impacts already affecting tropical forest biomass? *Global Environmental Change*, **14**, 299–302.
- Fujita D, Ishizawa M, Maksyutov S *et al.* (2003) Interannual variability of the atmospheric carbon dioxide concentrations as simulated with global terrestrial biosphere models and an atmospheric transport model. *Tellus*, **55B**, 530–546.
- Goulden ML, Miller SD, Rocha HR *et al.* (2004) Diel and seasonal patterns of tropical forest CO₂ exchange. *Ecological Applications*, **14**, S42–S54.
- Holland EA, Dentener FJ, Braswell BH *et al.* (1999) Contemporary and pre-industrial global reactive nitrogen budgets. *Biogeochemistry*, **46**, 7–43.
- Houghton RA (2003) Why are estimates of the terrestrial carbon balance so different? *Global Change Biology*, **9**, 500–509.

- Huete A, Didan K, Miura T *et al.* (2002) Overview of the radiometric and biophysical performance of the MODIS vegetation indices. *Remote Sensing of Environment*, **83**, 195–213.
- Huete AR, Didan K, Shimabukuro YE *et al.* (2006) Amazon rainforests green-up with sunlight in dry season. *Geophysical Research Letters*, **33**, L06405, doi: 10.1029/2005GL025583.
- Huete AR, Liu HQ, Batchily K *et al.* (1997) A comparison of vegetation indices over a global set of TM images for EOS-MODIS. *Remote Sensing of Environment*, **59**, 440–451.
- Hutyra LR, Munger JW, Nobre CA *et al.* (2005) Climatic variability and vegetation vulnerability in Amazonia. *Geophysical Research Letters*, **32**, L24712, doi: 10.1029/2005GL024981.
- Ichii K, Hashimoto H, Nemani RR *et al.* (2005) Modeling the interannual variability and trends in gross and net primary productivity of tropical forests from 1982 to 1999. *Global and Planetary Change*, **48**, 274–286.
- Jackson RB, Schenk HJ, Jobbagy EG *et al.* (2000) Belowground consequences of vegetation change and their treatment in models. *Ecological Applications*, **10**, 470–483.
- Jarvis PG (1976) The interpretation of the variations in leaf water potential and stomatal conductance found in canopies in the field. *Philosophical Transactions of the Royal Society of London Series B*, **273**, 593–610.
- Kalnay E, Kanamitsu M, Kistler R *et al.* (1996) The NCEP/NCAR 40-year reanalysis project. *Bulletin of the American Meteorological Society*, **77**, 437–471.
- Kleidon A (2004) Global datasets of rooting zone depth inferred from inverse methods. *Journal of Climate*, **17**, 2714–2722.
- Kleidon A, Heimann M (1998) A method of determining rooting depth from a terrestrial biosphere model and its impacts on the global water and carbon cycle. *Global Change Biology*, **4**, 275–286.
- Kobayashi H, Dye DG (2005) Atmospheric conditions for monitoring the long-term vegetation dynamics in the Amazon using normalized difference vegetation index. *Remote Sensing of Environment*, **97**, 519–525.
- Lee JE, Oliveira RS, Dawson TE *et al.* (2005) Root functioning modifies seasonal climate. *Proceedings of the National Academy of Sciences of the United States of America*, **102**, 17576–17581.
- Malhi Y, Pegoraro E, Nobre AD *et al.* (2002) Energy and water dynamics of a central Amazonian rain forest. *Journal of Geophysical Research*, **107**, 8061, doi: 10.1029/2001JD000623.
- Mitchell TD, Jones PD (2005) An improved method of constructing a database of monthly climate observations and associated high-resolution grids. *International Journal of Climatology*, **25**, 693–712.
- Nemani RR, Keeling CD, Hashimoto H *et al.* (2003) Climate-driven increases in global terrestrial net primary production from 1982 to 1999. *Science*, **300**, 1560–1563.
- Nepstad DC, de Carvalho CR, Davidson EA *et al.* (1994) The role of deep roots in the hydrological and carbon cycles of Amazonian forests and pastures. *Nature*, **372**, 666–669.
- Oliveira RS, Dawson TE, Burgess SSO *et al.* (2005) Hydraulic redistribution in three Amazonian trees. *Oecologia*, **145**, 354–363.
- Potter C, Davidson E, Nepstad D *et al.* (2001a) Ecosystem modeling and dynamic effects of deforestation on trace gas fluxes in Amazon tropical forests. *Forest Ecology and Management*, **152**, 97–117.
- Potter C, Klooster S, Carvalho CR *et al.* (2001b) Modeling seasonal and interannual variability in ecosystem carbon cycling for the Brazilian Amazon region. *Journal of Geophysical Research*, **106**, 10423–10446.
- Prentice IC, Farquhar GD, Fasham MJR *et al.* (2001) The carbon cycle and atmospheric carbon dioxide. In: *Climate Change 2001: The Scientific Basis. Contribution of Working Group I to the Third Assessment Report of the Intergovernmental Panel on Climate Change* (ed. Houghton JT *et al.*), pp. 183–237. Cambridge University Press, Cambridge.
- Roberts DA., Nelson BW, Adams JB *et al.* (1998) Spectral changes with leaf aging in Amazon caatinga. *Trees*, **12**, 315–325.
- Rocha HRD, Goulden ML, Miller SD *et al.* (2004) Seasonality of water and heat fluxes over a tropical forest in eastern Amazonia. *Ecological Applications*, **14**, S22–S32.
- Saleska SR, Miller SD, Matross DM *et al.* (2003) Carbon in Amazon forests: unexpected seasonal fluxes and disturbance-induced losses. *Science*, **302**, 1554–1557.
- Schenk HJ, Jackson RB (2002) The global biogeography of roots. *Ecological Monographs*, **72**, 311–328.
- Schenk HJ, Jackson RB (2005) Mapping the global distribution of deep roots in relation to climate and soil characteristics. *Geoderma*, **126**, 129–140.
- Schimel DS, House JI, Hibbard KA *et al.* (2001) Recent patterns and mechanisms of carbon exchange by terrestrial ecosystems. *Nature*, **414**, 169–172.
- Thornton PE, Law BE, Gholz HL *et al.* (2002) Modeling and measuring the effects of disturbance history and climate on carbon and water budgets in evergreen needleleaf forests. *Agricultural and Forest Meteorology*, **113**, 185–222.
- Vermote EF, El Saleous NZ, Justice CO (2002) Atmospheric correction of MODIS data in the visible to middle infrared: first results. *Remote Sensing of Environment*, **83**, 97–111.
- Vourlitis GL, Nogueira JS, Filho NP *et al.* (2005) The sensitivity of diel CO₂ and H₂O vapor exchange of a tropical transitional forest to seasonal variation in meteorology and water availability. *Earth Interactions*, **9**, 1–23.
- Williams M, Shimabukuro YE, Herbert DA *et al.* (2002) Heterogeneity of soil and vegetation in an eastern Amazonian rain forest: implications for scaling up biomass and production. *Ecosystems*, **5**, 692–704.
- Wilson KB, Baldocchi DD, Hanson AJ (2000) Spatial and seasonal variability of photosynthetic parameters and their relationship to leaf nitrogen in a deciduous forest. *Tree Physiology*, **20**, 565–578.
- Xiao X, Zhang Q, Saleska S *et al.* (2005) Satellite-based modeling of gross primary production in a seasonally moist tropical evergreen forest. *Remote Sensing of Environment*, **94**, 105–122.
- Zeng X, Dai YJ, Dickinson RE *et al.* (1998) The role of root distribution for land climate simulation. *Geophysical Research Letters*, **25**, 4533–4536.
- Zhang Y, Rossow WB, Lacis AA *et al.* (2004) Calculation of radiative fluxes from the surface to top of atmosphere based on ISCCP and other global data sets: refinements of the radiative transfer model and the input data. *Journal of Geophysical Research*, **109**, D19105, doi: 10.1029/2003JD004457.
- Zobler L (1986) *A World Soil File for Global Climate Modeling*, NASA Technical Memorandum 87802, NASA, 33 pp.